Theor Chem Acc (2006) 116: 281–296
DOI 10.1007/s00214-005-0042-8

REGULAR ARTICLE

Eric J. Bylaska

Estimating the thermodynamics and kinetics of chlorinated hydrocarbon degradation

Received: 19 April 2005 / Accepted: 27 September 2005 / Published online: 16 December 2005

Abstract Many different degradation reactions of chlorinated hydrocarbons are possible in natural groundwaters. In order to identify which degradation reactions are important, a large number of possible reaction pathways must be sorted out. Recent advances in ab initio electronic structure methods have the potential to help identify relevant environmental degradation reactions by characterizing the thermodynamic properties of all relevant contaminant species and intermediates for which experimental data are usually not available, as well as provide activation energies for relevant pathways. In this paper, strategies based on ab initio electronic structure methods for estimating thermochemical and kinetic properties of reactions with chlorinated hydrocarbons are presented. Particular emphasis is placed on strategies that are computationally fast and can be used for large organochlorine compounds such as 4,4′-DDT.

Keywords Chlorinated hydrocarbons · CCl_4 · DDT · PCE · TCE · DDT · Isodesmic reactions · Dissociative electron attachment reactions

1 Introduction

The widespread use of polychlorinated hydrocarbons (PCHs) as industrial solvents has resulted in their ubiquitous presence in the environment. The potential health risks to the public of these toxic and carcinogenic compounds being in the groundwater makes knowing their environmental fate extremely important. Due to their volatility, these toxic compounds are widely dispersed at low concentrations in the atmosphere [1]. In the subsurface, their immiscibility leads to pools and ganglia of nonaqueous phase liquid below a spill site, which then become a source for dissolved-phase contamination that can form a very large plume of contaminated groundwater [2]. This sort of contamination is difficult to remediate using conventional extraction technologies such as "pump and treat" [3,4], and, therefore, there is great interest in understanding degradation reactions that determine the environmental fate of chlorinated hydrocarbons.

Several chemical reactions have been hypothesized to contribute to the environmental degradation of PCHs including hydrogenolysis, dehydrochlorination, nucleophilic substitution, and hydrolysis [5,6]. One of the key degradation pathways for PCHs in anaerobic groundwater environments is reductive dechlorination (i.e., hydrogenolysis). This is one of the most studied reactions in environmental science because in-situ remediation strategies that degrade PCHs, whether they be chemical or microbiological, rely mainly on reductive reactions for dechlorination of the contaminants [5,7–18]. The hydrogenolysis mechanism involves two electrons and a proton and results in the formation of a chloride ion and of a new C–H bond.

$$\text{R–Cl} + 2e^- + H^+ \rightarrow \text{R–H} + Cl^- \quad (1)$$

This two electron-transfer reaction most likely occurs in two sequential steps. The first electron-transfer results in the dissociation of a chloride anion and the formation of a radical.

$$\text{R–Cl} + e^- \rightarrow R^\bullet + Cl^- \quad (2)$$

The second electron transfer leads to the protonation of the radical to form R–H.

$$R^\bullet + e^- + H^+ \rightarrow \text{R–H} \quad (3)$$

It is believed that the rate-limiting step in hydrogenolysis is the first electron reduction [(Eq. (2)]. For C_2 compounds, often in parallel with hydrogenolysis, especially above pH 8, dehydrochlorination may be significant, converting an alkane into an alkene.

$$HR_2C\text{–}CR_2Cl + OH^- \rightarrow R_2C{=}CR_2 + H_2O + Cl^- \quad (4)$$

This reaction is generally believed to occur by a bimolecular E2 elimination in which OH^- abstracts the proton away from

E.J. Bylaska
Fundamental Sciences Division,
Pacific Northwest National Laboratory,
P.O. Box 999, Richland,
WA 99352, USA.
E-mail: Eric.bylaska@pnl.gov

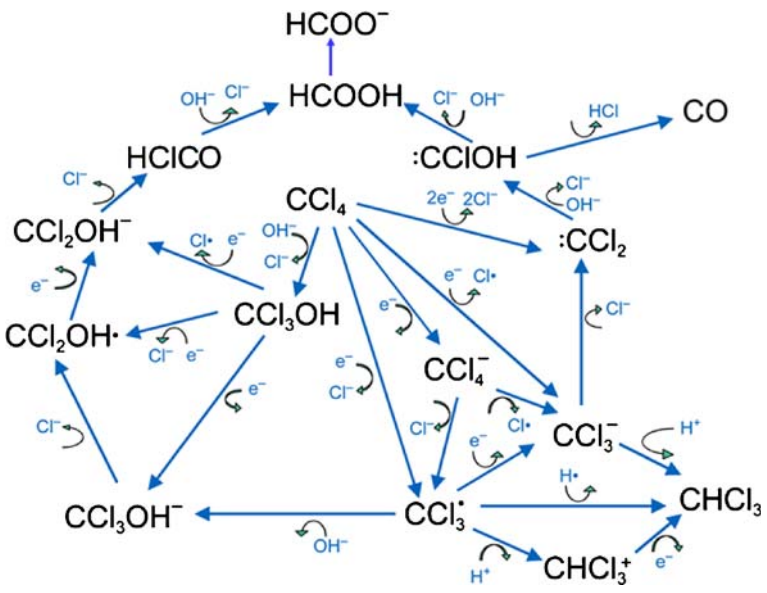

Fig. 1 Possible degradation reaction pathways for CCl_4

the central carbon with concerted loss of chloride from the trichloromethyl carbon [6,19].

In addition to reduction and elimination reactions, nucleophilic substitution reactions can lead to dechlorination by substitution with a variety of anions Nu^-; mainly OH^-, but also SH^-, HCO_3^-, F^-, etc.

$$R\text{–}Cl + Nu^- \rightarrow R\text{–}Nu + Cl^- \quad (5)$$

Previous work has shown that a wide variety of these dechlorinations by nucleophilic substitutions is thermodynamically favorable for simple chlorinated hydrocarbons such as CCl_4 [20,21]. Even if nucleophilic substitution reactions are expected to be slow in terms of kinetics and are not usually considered as degradation pathways, these reactions may become important on time scales relevant to groundwater systems [4,6]. In the case of OH^-, the nucleophilic substitution reaction, Eq. (6), results in an chloro-alcohol,

$$R\text{–}CCl_3 + OH^- \rightarrow R\text{–}CCl_2OH + Cl^- \quad (6)$$

$$R\text{–}CCl_2OH \rightarrow R\text{–}CCl(=O) + H^+ + Cl^- \quad (7)$$

$$R\text{–}CCl(=O) + OH^- \rightarrow R\text{–}COOH + Cl^- \quad (8)$$

and the subsequent reactions, Eqs. (7) and (8), which are expected to be fast, combine to produce a carboxylic acid [6].

As shown in Fig. 1, even for relatively simple chlorinated hydrocarbons such as CCl_4, an enormous number of reaction pathways are possible in natural groundwaters. In order to identify which degradation reactions are important, a large number of possible reaction pathways must be sorted out. There have been few detailed studies of these reactions, and many of the basic parameters (including thermodynamic heats of reaction, free energies of solvation, and kinetic rates) needed for a critical evaluation of reaction pathways are not known for a large number of chlorinated hydrocarbons, and obtaining all the needed basic parameters from experimental measurements will be an extremely laborious task. Ab initio electronic structure methods have the potential to help identify important environmental degradation reactions by characterizing the thermodynamic properties of all relevant contaminant species and intermediates for which experimental data is usually not available, and provide activation energies for relevant pathways.

Several groups have been applying computational chemistry methods to study the environmental degradation of simple and larger PCHs [20–38]. In this paper a brief account of strategies based on ab initio electronic structure methods currently being used for estimating the thermochemical properties of PCH degradation reactions is presented. Particular emphasis is placed on strategies that are computationally fast and can be used for large compounds such as 4,4′-DDT. We start by presenting strategies for estimating the thermodynamics (in the gas phase and aqueous solution) of PCHs and intermediates of hydrogenolysis, dehydrochlorination, nucleophilic substitution, and hydrolysis reactions, including the radicals, anions, and radical anions. Our focus is on obtaining accurate predictions of the enthalpies and free energies of reactions under ambient conditions. On the basis of these calculated thermodynamic estimates, the overall reaction energetics (in the gas phase and aqueous phase) can be determined. Equally important in understanding these reactions are the height and shape of activation barriers existing between the reactants and products. The large number of possible PCH degradation reactions precludes an all-inclusive discussion of methods for estimating the kinetics. Here we focus our discussion on a strategy currently being used by the author for estimating kinetics of the dissociative electron-transfer reaction, Eq. (2), which is the expected rate-limiting step in the hydrogenolysis. Finally, we conclude with a perspective on future directions.

2 Strategies for estimating thermodynamics

The main purpose of this section is to illustrate how computational chemistry methods can be used to estimate thermodynamics for reactions involving PCHs. The strategy discussed here for estimating the solution-phase reaction energies makes use of several different types of calculations including ab initio electron structure calculations, isodesmic reactions, gas-phase entropy estimates, and continuum solvations models. To estimate reaction energies separate computational steps are used to determine the electronic energy differences, entropy, and solvation. First the enthalpies of formation of all gas-phase species in the reaction are calculated followed by the calculation of their entropies. These combined calculations yield the gas-phase free energy. Then, the solvation energies of all species in the reaction are calculated. The solvation calculations account for the effect of solvent on gas-phase energetics. The desired results, reaction energies in both the gas phase and solution phase, can now be estimated because the necessary thermodynamic quantities are known either from experiment or obtained from the calculations described herein.

Strategies outlined in this section have been used by the author to estimate thermodynamic parameters, ΔH_f^o (298 K), S^o (298 K), and ΔG_s (298 K), for numerous PCHs including substituted chlorinated methanes, substituted chloromethyl radicals and anions, 4,4′-DDT and its metabolites, and polychloroethylene-yl radicals, anions, and radical anion complexes [20,22–24]. A partial compilation of this data is given in Tables 1–3.

2.1 Estimating $\Delta H_f^o(298\ K)$ using G2 methods and isodesmic reactions

The development of a computational scheme that can accurately predict the enthalpy of formation ΔH_f^o (298 K) requires some care. The most basic strategy in which ΔH_f^o (298 K) is determined by directly calculating the atomization energy only works when very large basis sets such as the correlation-consistent basis sets, high-level treatments of correlation energy such as coupled cluster methods (CCSD(T)) [39–41], and small correction factors such as core-valence correlation energies and relativistic effects are included in the ab initio electronic structure calculation. Even though high-level ab initio electronic structure calculations have been shown to be able to estimate ΔH_f^o (298 K) of small halogenated [30] and other molecules [40,42–47] within a few kcal/mol, these methods are extremely demanding, scaling at least as N^7 for N basis functions, and are currently limited to molecules of up to eight first-row atoms.

In contrast, lower-level ab initio (i.e., Hartree–Fock, MP2) and Density Functional Theory [48,49] calculations (i.e., LDA [50], BPW91 [51,52], PBE96 [53], PBE0 [54], and B3LYP [55,56]) are much more computationally efficient and can be used to calculate a wide class of molecules containing hundreds of atoms on modest computational resources. Unfortunately, such lower-level calculations cannot be used to directly calculate ΔH_f^o (298 K) using atomization energies because these calculations have large errors. Examples of directly calculating ΔH_f^o (298 K) using low-level theories are shown in Table 4. Calculated in this way the differences found between the different levels of ab initio theory are very large. These examples demonstrate that care must be taken in choosing the appropriate method for calculating heats of formation from total atomization energies.

A number of phenomenological approaches have been developed to improve the accuracy of lower-level ab initio and density functional theory methods. In general all these approaches make use of empirical additivity rules for molecular properties. As pointed out by Benson in his classical book Thermochemical Kinetics [57], it has been known for some time that a number molecular properties of larger molecules, including its refractive index, UV and IR absorption, magnetic susceptibility, entropy, molar heat capacity, and heats of formation, can be thought of as being roughly made up of additive contributions of atoms, bonds, or collections of atoms and bonds (i.e., functional groups) of the molecule. The physical basis of such an empirical finding is not completely clear, however, it has been speculated to be a consequence of the fact that the forces between additive groups in the same or different molecules are very short range and rarely extend beyond a few angstroms.

One popular approach for estimating enthalpies of formation ΔH_f^o (298 K) of covalently bonded molecules is the G2 method of Curtis et al. [58,59] and the subsequent variants G2(MP2), G3 [60], and G3(MP2). The G2 classes of methods correct errors associated with the calculation atomization energies by using an additivity correction scheme. These calculations are still computationally very intensive, but molecules containing as many as 15–20 first- and second-row atoms can be computed. The accuracy of G2 methods which contain empirical parameters is quite good, reproducing atomization energies to usually within a few kcal/mol for many molecules as shown in the sixth column of Table 1. However, even at the G2 level, it is not always possible to calculate the heat of formation to within ±1 kcal/mol and other methods can have even more difficulty. For example, the G2 value for ΔH_f (CF_4) at 0 K is −227.2 kcal/mol [58] as compared to the JANAF value of −221.6 ± 0.3 kcal/mol [61], an error of 5.6 kcal/mol. Similarly, the G2 value for ΔH_f (C_2F_4) at 0 K is –164.8 kcal/mol [58], compared to the experimental value of −157.5 ± 0.7 kcal/mol [61], an error of 8.2 kcal/mol. It is useful to note that the G2 values are more negative (higher atomization energy) than the experimental ones. However, the G2 method is significantly better than many other methods for calculating heats of formation based on atomization energies.

Another standard approach for estimating enthalpies of formation ΔH_f^o (298 K) is to use isodesmic reaction schemes. This strategy is computationally tractable for large molecules and is usually accurate to within a few kcal/mol. Isodesmic reactions are (hypothetical) chemical reactions in which there are an equal number of like bonds (of each formal type) on

Table 1 Gas-phase thermodynamic parameters from isodesmic reaction and G2 calculations for the substituted chlorinated methanes[a,b,c]

C1 compounds	ΔH_f^o(298.15 K) (kcal/mol) (isodesmic)				ΔH_f^o(298.15 K) (atomization)	ΔH_f^o(298.15 K) (exp)
	LDA/ DZVP2	BP91/ DZVP2	B3LYP/ DZVP2	MP2/ cc-pVDZ	G2	
CCl_3F	−72.35	−68.57	−67.10	−69.43	−72.50	−69.00[e]
CCl_2HF	−70.15	−67.10	−65.76	−63.97		−67.70[e]
$CClH_2F$	−64.36	−62.61	−61.72	−54.96	−65.11	−62.60[e]
CH_3F					−58.23	−56.00[e]
CCl_3OH	−69.21	−65.15	−64.01	−69.43	−68.35	
$CHCl_2OH$	−64.36	−62.60	−61.62	−63.97	−64.16	
CH_2ClOH	−54.87	−54.09	−53.70	−54.96	−59.79	
CH_3OH					−49.26	−47.96[g]
CCl_3SH	−11.86	−8.68	−7.64	−13.40	−12.95	
$CHCl_2SH$	−11.07	−8.66	−7.92	−11.48	−11.52	
CH_2ClSH	−6.66	−5.44	−5.20	−7.01	−6.98	
CH_3SH					−4.76	−5.34[g]
CCl_3 (HCO_3)	−149.97	−145.53	−144.09	−150.79		
$CHCl_2$ (HCO_3)	−153.70	−150.73	−149.45	−154.11		
CH_2Cl (HCO_3)	−150.33	−148.53	−147.59	−149.82		
CH_3 (HCO_3)					−144.61	−145.1[o]
	S° (cal/mol-K)					S° (cal/mol-K) (exp)
	LDA/ DZVP2	BP91/ DZVP2	B3LYP/ DZVP2	MP2/ cc-pVDZ		
CCl_3F	74.143	74.594	74.205	73.688		74.030[e]
CCl_2HF	70.139	70.436	70.184	69.850		70.088[e]
$CClH_2F$	63.222	63.393	63.260	63.082		63.196[e]
CH_3F	53.262	53.324	53.258	53.202		53.260[e]
CCl_3OH	78.053	78.412	77.967	77.123		
$CHCl_2OH$	72.066	72.269	72.017	71.356		
CH_2ClOH	63.162	63.3289	63.205	63.029		
CH_3OH	57.073	57.101	57.068	56.706		57.316[g]
CCl_3SH	81.348	81.673	81.220	80.514		
$CHCl_2SH$	75.456	75.691	75.241	74.700		
CH_2ClSH	69.745	71.979	69.978	68.886		
CH_3SH	60.618	60.630	60.614	60.409		60.987[g]
CCl_3 (HCO_3)	99.217	100.066	99.307	98.535		
$CHCl_2$ (HCO_3)	95.504	96.130	95.573	95.027		
CH_2Cl (HCO_3)	88.022	88.515	88.105	87.684		
CH_3 (HCO_3)	78.362	78.632	78.230	78.039		
	ΔG_S(kcal/mol)[d]					
	LDA/ DZVP2	BP91/ DZVP2	B3LYP/ DZVP2	MP2/ cc-pVDZ		
CCl_3F	4.72	4.88	4.80	4.64		2.73[h]
CCl_2HF	1.28	1.11	1.21	0.92		0.98[i]
$CClH_2F$	0.40	0.44	0.23	0.07		1.12[i]
CH_3F	1.62	1.66	1.43	1.45		1.57[i]
CCl_3OH	−2.15	−1.71	−1.79	−1.36		
$CHCl_2OH$	−5.96	−5.49	−5.58	−6.03		
CH_2ClOH	−6.79	−6.24	−6.48	−6.35		
CH_3OH	−3.65	−3.19	−3.34	−2.81		−3.19[j]
CCl_3SH	2.72	3.05	3.16	2.92		
$CHCl_2SH$	−0.37	−0.06	0.3	−0.28		
CH_2ClSH	−1.37	−1.06	−1.08	−1.14		
CH_3SH	0.42	0.64	0.71	0.74		
CCl_3 (HCO_3)	−3.68	−2.80	−3.13	−3.77		
$CHCl_2$ (HCO_3)	−4.57	−3.85	−5.43	−4.60		
CH_2Cl (HCO_3)	−7.30	−6.51	−7.05	−7.47		
CH_3 (HCO_3)	−5.66	−5.26	−5.65	−5.56		

[a] All values used in this table were taken from [20]
[b] DZVP2 [104] basis set used for LDA, BPW91, and B3LYP; cc-pVDZ [105–110] basis set used for MP2
[c] All calculations in this table used the Gaussian98 program package [65]
[d] PCM model calculations [70–73] with cavity defined by united atom model [111]
[e] Experimental reference [112]
[o] Experimental reference [113]
[g] Experimental reference [88]
[h] Experimental reference [114]
[i] Experimental reference [115]
[j] Experimental reference [116]

Table 2 Gas-phase thermodynamic parameters from isodesmic reaction and G2 calculations for the substituted chlorinated methyl radicals [a,b,c]

C1 radicals	ΔH_f^o(298.15 K) (kcal/mol) (isodesmic)					ΔH_f^o(298.15 K) (atomization)	ΔH_f^o(298.15 K) (exp)
	LDA/ DZVP2	BP91/ DZVP2	B3LYP/ DZVP2	MP2/ cc-pVDZ	G2	G2	
$CCl_3^\bullet$	11.57	14.54	16.12	18.42	17.15	17.45	14.1 . . . 19.12[e]
$CHCl_2^\bullet$	16.68	20.42	21.82	23.50	21.82	21.74	21.27 . . . 28.2[e]
$CH_2Cl^\bullet$	24.66	27.19	28.10	28.40	27.61	27.63	24.14 . . . 31.31[e]
$CCl_2F^\bullet$	−27.48	−25.07	−23.30	−21.75	−21.84	−23.50	−22 . . . 25.10[e]
$CHClF^\bullet$	−20.64	−17.74	−16.19	−15.64	−15.18	−16.69	−14.51 . . . − 15[e]
$CH_2F^\bullet$	−10.71	−8.39	−7.36	−7.54	−6.35	−7.58	−7.65 . . . − 8[e]
$CCl_2OH^\bullet$	−26.83	−24.13	−22.45	−20.60	−22.21	−21.40	
$CHClOH^\bullet$	−18.24	−14.93	−13.33	−12.45	−8.38	−12.20	
$CH_2OH^\bullet$	−8.56	−5.59	−4.61	−4.04	−3.36	−3.65	2 ± 1[e]
$CCl_2SH^\bullet$	22.44	26.11	27.82	29.30	28.76	29.72	
$CHClSH^\bullet$	27.68	31.45	33.01	35.24	33.68	34.71	
$CH_2SH^\bullet$	33.80	36.41	37.28	40.12	38.26	39.84	
$CCl_2(HCO_3)^\bullet$	−112.49	−109.55	−107.84	−104.89	−106.20	−104.63	
$CHCl(HCO_3)^\bullet$	−107.89	−105.12	−103.55	−101.37	−102.01	−100.51	
$CH_2(HCO_3)^\bullet$	−101.96	−99.97	−98.70	−96.37	−96.05	−98.56	
	S° (cal/mol-K)						S° (cal/mol-K) (exp)
	LDA/ DZVP2	BP91/ DZVP2	B3LYP/ DZVP2	MP2/ cc-pVDZ			
$CCl_3^\bullet$	71.99	72.19	72.12	71.61			70.94[o]
$CHCl_2^\bullet$	63.56	63.71	63.66	63.53			
$CH_2Cl^\bullet$	58.68	60.54	61.80	57.05			
$CCl_2F^\bullet$	71.29	71.55	71.35	71.03			
$CHClF^\bullet$	64.14	64.24	64.14	63.96			
$CH_2F^\bullet$	56.87	56.51	56.41	56.11			
$CCl_2OH^\bullet$	71.43	71.678	71.48	71.09			
$CHClOH^\bullet$	66.03	66.15	65.99	65.51			
$CH_2OH^\bullet$	57.90	57.57	57.49	57.08			
$CCl_2SH^\bullet$	78.11	78.07	78.08	75.93			
$CHClSH^\bullet$	70.29	70.19	69.86	69.34			
$CH_2SH^\bullet$	63.56	60.59	60.51	61.37			
$CCl_2(HCO_3)^\bullet$	88.05	88.86	88.24	87.46			
$CHCl(HCO_3)^\bullet$	81.56	82.41	82.05	81.77			
$CH_2(HCO_3)^\bullet$	73.90	72.86	72.60	73.03			
	ΔG_S(kcal/mol)[d]						
	LDA/ DZVP2	BP91/ DZVP2	B3LYP/ DZVP2	MP2/ cc-pVDZ			
$CCl_3^\bullet$	4.44	4.68	4.60	4.30			
$CHCl_2^\bullet$	1.86	1.91	1.85	1.04			
$CH_2Cl^\bullet$	1.81	1.71	1.66	1.29			
$CCl_2F^\bullet$	4.04	4.15	4.03	3.72			
$CHClF^\bullet$	0.58	0.66	0.50	−0.02			
$CH^2F^\bullet$	1.03	1.03	0.86	0.79			
$CCl_2OH^\bullet$	−2.91	−2.30	−2.40	−2.35			
$CHClOH^\bullet$	−5.93	−5.23	−5.39	−5.47			
$CH_2OH^\bullet$	−4.16	−3.44	−3.53	−2.95			
$CCl_2SH^\bullet$	2.36	2.60	2.59	2.27			
$CHClSH^\bullet$	−0.87	−0.51	−0.46	−0.87			
$CH_2SH^\bullet$	−0.20	0.13	0.21	0.18			
$CCl_2(HCO_3)^\bullet$	−3.56	−2.59	−2.71	−4.13			
$CHCl(HCO_3)^\bullet$	−6.04	−5.22	−5.74	−6.18			
$CH_2(HCO_3)^\bullet$	−5.36	−4.62	−5.00	−5.33			

[a] All values used in this table were taken from [23]
[b] DZVP2 [104] basis set used for LDA, BPW91, and B3LYP; cc-pVDZ [105–110] basis set used for MP2
[c] All calculations in this table used the Gaussian98 program package [65]
[d] PCM model calculations [70–73] with cavity defined by united atom model [111]
[e] See [23] for listing of experimental values
[o] Experimental reference [112]

Table 3 Gas-phase thermodynamic parameters from isodesmic reactions and G2 calculations for the polychlorinated ethylene radicals and DDT compounds[a,b,c,d]

C_2 radicals	ΔH_f^o(298.15 K) (kcal/mol) (isodesmic) LDA/6-311 ++G(2*d*,2*p*)	PBE96/6-311 ++G(2*d*,2*p*)	B3LYP/6-311 ++G(2*d*,2*p*)	MP2/6-311 ++G(2*d*,2*p*)	RCCSD(T)/ aug-cc-pVTZ	G2	ΔH_f^o(298.15 K) atomization G2
$C_2Cl_3^\bullet$	53.20	52.69	53.20	58.35	55.28	54.56	56.17
trans-$C_2HCl_2^\bullet$	58.29	58.31	58.86	62.32	59.98	59.30	60.55
cis-$C_2HCl_2^\bullet$	57.74	57.29	57.78	61.57	59.29	58.67	58.76
1, 1-$C_2HCl_2^\bullet$	62.52	61.68	61.60	64.45	62.74	62.63	63.63
trans-$C_2H_2Cl^\bullet$	67.76	66.91	66.71	68.21	67.42	67.32	67.13
cis-$C_2H_2Cl^\bullet$	68.84	68.24	68.08	69.25	68.50	68.38	68.19
1, 1-$C_2H_2Cl^\bullet$	62.62	62.82	63.51	65.57	64.22	63.61	63.42
S° (cal/mol-K)							
$C_2Cl_3^\bullet$	79.94	80.13	79.70	78.50			
trans-$C_2HCl_2^\bullet$	72.40	72.47	72.19	71.40			
cis-$C_2HCl_2^\bullet$	72.48	72.55	72.24	71.57			
1, 1-$C_2HCl_2^\bullet$	72.27	72.29	71.85	71.03			
trans-$C_2H_2Cl^\bullet$	64.78	64.83	64.48	63.98			
cis-$C_2H_2Cl^\bullet$	64.76	64.66	64.29	63.73			
1, 1-$C_2H_2Cl^\bullet$	64.04	64.12	63.92	63.53			
ΔG_{SCRF}(kcal/mol)[e]							
$C_2Cl_3^\bullet$	4.89	5.07	5.02	4.81			
trans-$C_2HCl_2^\bullet$	2.75	2.95	2.94	2.86			
cis-$C_2HCl_2^\bullet$	3.06	3.23	3.23	2.83			
1, 1-$C_2HCl_2^\bullet$	3.71	3.86	3.79	3.47			
trans-$C_2H_2Cl^\bullet$	2.04	2.22	2.19	2.14			
cis-$C_2H_2Cl^\bullet$	1.70	1.91	1.89	1.85			
1, 1-$C_2H_2Cl^\bullet$	3.46	3.60	3.65	3.51			

DDT compounds	ΔH_f^o(298.15 K) (kcal/mol) Isodesmic LDA/ DZVP2	PBE96/ DZVP2	B3LYP/ DZVP2	PBE0/ DZVP2	MP2/ cc-pVDZ
$(C_6H_4Cl)_2$–CH–CCl_3	10.37	15.39	17.32	16.91	5.66
$(C_6H_4Cl)_2$–CH–CCl_2H	12.79	16.52	17.74	17.90	7.60
$(C_6H_4Cl)_2$–CH–$CCl_2^\bullet$	54.95	58.34	59.85	60.02	
$(p\text{-}C_6H_4Cl)_2$–C=CCl_2	35.38	38.88	40.55	40.85	32.88
$(p\text{-}C_6H_4Cl)_2$–CH–CCl_2OH	−32.06	−26.12	−24.14	−24.60	−36.24
$(p\text{-}C_6H_4Cl)_2$–CH–CCl(=O)	−16.33	−13.74	−13.08	−12.12	−19.97
$(p\text{-}C_6H_4Cl)_2$–CH–COOH	−60.41	−58.04	−57.32	−56.33	−63.56

	S° (cal mol^{-1} K^{-1}) LDA/ DZVP2	PBE96/ DZVP2	B3LYP/ DZVP2	PBE0/ DZVP2
$(C_6H_4Cl)_2$–CH–CCl_3	140.592	141.303	138.892	138.126
$(C_6H_4Cl)_2$–CH–CCl_2H	137.068	138.746	136.902	136.747
$(C_6H_4Cl)_2$–CH–$CCl_2^\bullet$	137.028	136.795	135.349	134.621
$(p\text{-}C_6H_4Cl)_2$–C=CCl_2	138.383	139.746	138.416	137.707
$(p\text{-}C_6H_4Cl)_2$–CH–CCl_2OH	134.911	134.843	133.59	133.112
$(p\text{-}C_6H_4Cl)_2$–CH–CCl (= O)	137.259	138.255	136.346	135.963
$(p\text{-}C_6H_4Cl)_2$–CH–COOH	135.365	136.979	134.779	134.686

	ΔG_S(kcal/mol)[e] LDA/ DZVP2	PBE96/ DZVP2	B3LYP/ DZVP2	PBE0/ DZVP2
$(C_6H_4Cl)_2$–CH–CCl_3	−6.12	−5.62	−5.18	−5.58
$(C_6H_4Cl)_2$–CH–CCl_2H	−11.76	−11.05	−10.61	−10.99
$(C_6H_4Cl)_2$–CH–$CCl_2^\bullet$	−6.96	−6.32	−5.90	−6.24
$(p\text{-}C_6H_4Cl)_2$–C=CCl_2	1.31	1.42	1.36	1.22
$(p\text{-}C_6H_4Cl)_2$–CH–CCl_2OH	−10.61	−10.97	−10.97	−11.02
$(p\text{-}C_6H_4Cl)_2$–CH–CCl(=O)	−6.65	−5.72	−6.02	−5.95
$(p\text{-}C_6H_4Cl)_2$–CH–COOH	−12.83	−12.48	−11.50	−11.90

[a] All values used in this table were taken from [22,24]
[b] NWChem program package [64] used for DFT calculations; Molpro program package used for RCCSD(T) calculations; Gaussian 98 program package [65] used for G2 calculations
[c] 6-311++G(2*d*,2*p*) [117,118] basis set used for LDA, PBE96, B3LYP, and MP2; aug-cc-pVTZ [105] basis set used for RCCSD(T)
[d] DZVP2 [104] basis set used for LDA, PBE96, B3LYP, and PBE0; cc-pVDZ [105–110] basis set used for MP2
[e] COSMO model calculations [74] with cavity defined by united atom model [111]

Table 4 Gas-phase enthalpies of formation estimates based on atomization energies[a]

	ΔH_f^o(298.15 K) (kcal/mol) (atomization)					ΔH_f^o(298.15 K) (exp)
C1 radicals	LDA/ DZVP2	BP91/ DZVP2	B3LYP/ DZVP2	MP2/ cc-pVDZ	G2	
$CCl_3^\bullet$	−31.84	16.85	40.44	41.59	17.45	14.1 . . . 19.12[b]
$CHCl_2^\bullet$	−22.07	21.79	36.89	48.22	21.74	21.27. . .28.2[b]
$CH_2Cl^\bullet$	−8.47	29.66	36.42	55.09	27.63	24.14. . .31.31[b]
$CH_2OH^\bullet$	−64.90	−0.17	5.17	34.48	−3.65	2±1[b]
C2 radicals	LDA/6-311 6-311++G(2*d*,2*p*)	PBE96/6-311 6-311++G(2*d*,2*p*)	B3LYP/6-311 6-311++G(2*d*,2*p*)	MP2/6-311 6-311++G(2*d*,2*p*)	G2	
$C_2Cl_3^\bullet$	−33.87	34.52	75.90	76.70	56.17	
trans-$C_2HCl_2^\bullet$	−18.31	43.33	74.30	83.37	60.55	
cis-$C_2HCl_2^\bullet$	−20.60	41.25	72.48	81.31	58.76	
	LDA/ DZVP2	PBE96/ DZVP2	B3LYP/ DZVP2	PBE0/ DZVP2		
$(C_6H_4Cl)_2$–CH–$CCl_2^\bullet$	−395.53	4.76	175.25	72.60		

[a] ab initio total energy values used to determine these enthalpies of formations can be found in the supplementary material of references [22–24]
[b] See [23] for listing of experimental values

the left- and right-hand sides of the reaction. Examples of isodesmic reactions that have been used to estimate thermochemical properties of several chlorinated hydrocarbons and degradation reaction intermediates are

$$CH_3L + CH_{x+1}Cl_{3-x} \rightarrow CH_xCl_{3-x}L + CH_4 \quad (9)$$

$$CH_{x+1}Cl_{2-x}L + CH_3^\bullet \rightarrow CH_xCl_{2-x}L^\bullet + CH_4 \quad (10)$$

$$CH_{x+1}Cl_{2-x}L + CH_3^- \rightarrow CH_xCl_{2-x}L^- + CH_4 \quad (11)$$

$$C_2H_{x+1}Cl_{3-x} + C_2H_3^\bullet \rightarrow C_2H_xCl_{3-x}^\bullet + C_2H_4, \quad (12)$$

$$C_2H_{x+1}Cl_{3-x} + C_2H_3^- \rightarrow C_2H_xCl_{3-x}^- + C_2H_4, \quad (13)$$

where $L^- = F^-, OH^-, SH^-, NO_3^-, HCO_3^-$, and $x = 0, 1, 2$. For larger molecules it is sometimes necessary to use more complicated isodesmic reactions. For example, the thermochemical properties of DDT compounds were estimated using

$$(p\text{-}C_6H_4Cl)_2\text{–}R + 2C_6H_6 + CH_4 \rightarrow (C_6H_5)_2\text{–}CH_2 + 2C_6H_5Cl + H_2R \quad (14)$$

with $R \equiv$ =CH–CCl_3, =CH–$CCl_2^\bullet$, =CH–$CHCl_2$, =C=CCl_2, =CH–CCl_2OH, =CH–CCl(=0) and =CH–COOH

Isodesmic reactions are designed to separate out the interactions between the additive functional groups and nonbonding electrons from the direct-bonding electrons by having the direct-bonding interactions largely canceling one another. This separation is quite attractive. Most low-level ab initio methods give substantial errors when estimating direct-bonding interactions due to the computational difficulties associated with electron pair correlation, whereas low-level ab initio methods are expected to be more accurate for estimating neighboring interactions and long-range through-bond effects.

To estimate the enthalpy of formation ΔH_f^o (298 K) of a compound the following approach based on isodesmic reactions may be used:

1. "Invent" an isodesmic reaction which contains the unknown compound whose ΔH_f^o (298 K) is needed and other simple compounds whose ΔH_f^o (298 K) are known.
2. Calculate the reaction enthalpy of the isodesmic reaction from the electronic, thermal, and vibrational energy differences at 298.15 K at a consistent level of theory.
3. The enthalpy of formation of the unknown compound is then backed out by using Hess's law with the calculated reaction enthalpy and the known enthalpies of formation of the other compounds.

In order to illustrate this strategy, we estimate ΔH_f^o (298 K) for the radical $C_2Cl_3^\bullet$ using an isodesmic reaction scheme. First, the reaction enthalpy for the following isodesmic reaction containing $C_2Cl_3^\bullet$ (i.e., Eq. (12), $x = 0$),

$$C_2HCl_3 + C_2H_3^\bullet \overset{\Delta H_{rxn}^{isodesmic}}{\rightarrow} C_2Cl_3^\bullet + C_2H_4 \quad (15)$$

is calculated from the electronic, thermal, and vibrational energy differences at 298.15 K at a consistent level theory. Computed values for ΔH_{rxn} at various levels of electronic structure theory are −0.69, −1.20, −0.69, 4.46, and 0.67 kcal/mol, respectively for the SVWN5/6-311++G(2*d*,2*p*), PBE96/6-311++G(2*d*,2*p*), B3LYP/6-311++G(2*d*,2*p*), MP2/6-311++ G (2*d*,2*p*), and G2 levels. Given that ΔH_f^o (298 K) of the other three species are known from experiment ($\Delta H_f^o C_2HCl_3$ = 7.0 kcal/mol, $\Delta H_f^o C_2H_3^\bullet$ = 71.0 kcal/mol, $\Delta H_f^o C_2H_4$ = 12.5 kcal/mol). ΔH_f^o (298 K) of the unknown $C_2Cl_3^\bullet$ compound is calculated using Hess's law.

$$\Delta H_f^o C_2Cl_3^\bullet = \Delta H_f^o C_2H_3^\bullet + \Delta H_f^o C_2HCl_3 - \Delta H_f^o C_2H_4 + \Delta H_{rxn}^{isodesmic} \quad (16)$$

Results for ΔH_f^o (298 K) at different levels of theory are given in Table 3. This method is simple to apply as long as selected enthalpies of formation of the $C_2H_3^\bullet$, C_2H_4, and C_2HCl_3 are known either from experiment or high-quality ab initio estimates.

The success of the isodesmic strategy is controlled by several factors, including the accuracy of ΔH_f^o (298 K) for

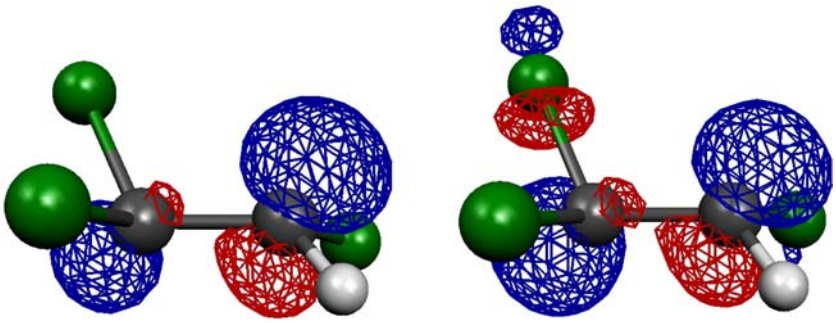

Fig. 2 Highest occupied molecular orbital (*left* ROHF/6-311++G(2*d*,2*p*) calculation, *right* LSDA/6-311++G(2*d*,2*p*) calculation) for π^* structure of $C_2HCl_3^-$

the reference species, the level of the ab initio theory, the size of basis set used to calculate the electronic energy difference, and the accuracy of the molecular vibration corrections. One should also bear in mind that it is often possible to use several different isodesmic reactions to estimate the enthalpy of formation of the same species. These different isodesmic reactions will give slightly different results (hopefully small), and there is no way to know a priori if one reaction is necessarily better than another.

It should be mentioned that for some radical species unrestricted ab initio theories may fail. In particular, unrestricted Hartree–Fock (UHF) theory and unrestricted MP2 theory often produce fictitious states with a significant amount of spin contamination. Such fictitious states do not give reliable energetics and should not be used in isodesmic estimates. For example, UMP2 calculations for the DDT radical species $(C_6H_4Cl)_2$–CH–$CCl_2^{\bullet}$ contain a significant amount of spin contamination (S^2 =1.14 compared to an ideal value of S^2 =0.75), and estimating ΔH_f^o (298 K) using Eq. (14) resulted in an inaccurate answer (95.27 kcal/mol at the UMP2 level compared to 59.48 kcal/mol at the B3LYP level). When such problems occur, restricted open shell theories should be used in place of unrestricted open shell theories. In general, unrestricted density functional theory calculations do not suffer from these problems. However, there are several known examples where UDFT also predicts a significant amount of spin contamination. An example of an UDFT failure is seen for the π^* structure of the $C_2HCl_3^{-\bullet}$. Using UDFT and UHF, a stable π^* structure is not found and the optimization always results in a σ^* structure (i.e., C_2HCl_2–Cl^- structure). We attribute this to the spin contamination. As shown in Fig. 2, the ROHF→UHF instability results in a highest occupied molecular orbital that contains a significant amount of symmetry-breaking mixing between the π^*-like and σ^*_{c-cl} orbitals, which in turn results in an unstable structure. Only by using ROHF we are able to attain a stable π^* structure.

2.2 Estimating thermodynamic functions

Given an optimized structure and vibrational frequencies for a gas-phase polyatomic molecule, one can calculate various thermodynamic functions using formulae derived from statistical mechanics [62,63]. In many cases, results from these formulae, with accurate structures and frequencies, will often provide more accurate values than those determined by direct thermal measurements. Calculation of these formulae is straightforward and many ab initio electronic structure programs [64,65] contain options for calculating these formulae.

For many chlorinated hydrocarbons these formulae have been found to work well. However, for molecules with hindered rotations [62,63], the situation is considerably more complicated. In these kinds of molecules, e.g., ethane, one of the most important internal degrees of freedom is the rotation of one fragment of a molecule relative to the rest about a single bond connecting the two parts. There are two limiting cases for this kind of rotation. The first is that the barrier impeding the rotation of the functional group is very high. The second is that the rotation about the single bond is essentially unhindered. For extremely hindered rotations, the functional group will not rotate except at extremely high temperatures. In this case, the rotation can be considered as a torsional oscillation at ambient temperatures and thus can be treated as a regular vibration in its contribution to the partition function. However, for temperature ranges where there is nearly free rotation (the second limiting case), one must treat the contribution to the partition function in a different way. In order to calculate accurate thermodynamic functions for molecules with nearly unhindered internal bond rotations, a contribution due to each internal bond rotation needs to be added. Although there are several ways to do this, the expressions of Pitzer and Gwinn [62,66,67], which assume that the bond rotations are unhindered, work well in many cases. In spite of the simplicity of this approximation, it has been demonstrated that this assumption only slightly overestimates the entropy of a hindered bond rotation.

A more direct way to handle hindered rotations is to explicitly solve for the energy levels of the rotational Schrödinger equation of each rotor and then use this as input into a canonical partition function of the bond rotation. The rotational Schrödinger equation for a rotor is written as [63, 68]

$$\frac{-\hbar^2}{2I_r}\frac{\partial^2\psi}{\partial^2\varphi} + V(\varphi)\psi = \varepsilon\psi \tag{17}$$

where I_r is the reduced moment of inertia, and $V(\phi)$ is the rotational potential. For molecules containing a single top attached to a rigid frame, the reduced moment of inertia is [62,66]

$$I_r = I_{top}\left[1 - I_{top}\left(\frac{\lambda_{top-A}}{I_A} + \frac{\lambda_{top-B}}{I_B} + \frac{\lambda_{top-C}}{I_C}\right)\right] \quad (18)$$

with I_{top} the moment of inertia of the top itself, λ_{top-A} the cosine of the angle between the axis of the top and the axis of the principle moment of inertia I_A of the whole molecule, and λ_{top-B} and λ_{top-C} the projections of the top axis onto the axes of the other principle moments of inertia I_B and I_C. The rotational potential energy surface, $V(\phi)$, can be mapped out using electronic structure energy calculations in $d\theta$ rotating increments ($360°/d\theta$ points). The energy levels of the rotational Schrödinger equation can be solved in a variety of ways [69]. In a previous work [22] we found that the Eq. (21) could readily be solved by fast Fourier transforming the extended rotational potential energy surface

$$\tilde{V}(k) = \frac{1}{N}\sum_{i=0}^{N-1} V(i) e^{i\frac{2\pi jk}{N}} \quad (19)$$

and then diagonalizing the following Hamiltonian matrix using N points (high-frequency modes of the rotational potential energy surface can be set to zero by linearly interpolating $V(\phi)$ to use N points).

$$H(i,j) = \begin{cases} \frac{1}{2I_r} i^2 \delta_{i,j} + \tilde{V}(\mathrm{mod}\,[i-j,N]), & \text{for } 0 \le i \le \frac{N}{2},\ 0 \le j \le \frac{N}{2} \\ \tilde{V}(\mathrm{mod}\,[i-j+N,N]), & \text{for } 0 \le i \le \frac{N}{2},\ \frac{N}{2} < j < N \\ \tilde{V}(\mathrm{mod}\,[i-N-j,N]), & \text{for } \frac{N}{2} < i < N,\ 0 \le j \le \frac{N}{2} \\ \frac{1}{2I_r}(i-N)^2 \delta_{i,j} + \tilde{V}(\mathrm{mod}\,[i-j,N]) & \text{for } \frac{N}{2} < i < N,\ \frac{N}{2} < j < N \end{cases} \quad (20)$$

to obtain rotational energy levels, ε_i. A large number of rotational levels ($N > 1{,}000$) are needed to ensure that the calculation of the canonical partition function is converged.

The entropy and internal energy correction of the rotor is then calculated by using the following formulae [62].

$$Q_{rotor} = \frac{\sum_{i=0}^{N-1} e^{-\frac{\varepsilon_i}{RT}}}{\sigma} \quad (21)$$

$$U_{rotor} = RT^2 \frac{d(\ln Q_{rotor})}{dT} \quad (22)$$

$$S^o_{rotor} = R \ln Q_{rotor} + RT \frac{d(\ln Q_{rotor})}{dT} \quad (23)$$

where σ is the number of indistinguishable positions of the rotor (e.g., $\sigma = 3$ for the $R_1 = CCl_3$ rotor).

2.3 Estimating solvation energies

Solvent effects can be estimated by using the self-consistent reaction field (SCRF) theories of Tomasi et al. (PCM) [70–73] or Klampt and Schüürmann (COSMO) [74]. SCRF theory can be combined with a variety of ab initio electronic structure calculations, including DFT with the LDA, BP91, and B3LYP functionals, and MP2. Despite the approximate treatment of solvation in this approach, it and others like it have been shown to give hydration energies of many neutral molecules within a few kcal/mol as compared to experiment [70,73,75–79].

In SCRF theory the solvation energies for rigid solutes that do not react strongly with water are approximated as a sum of noncovalent electrostatic, cavitation, and dispersion energies. Several ways have been proposed to calculate these contributions. For the electrostatic energy, the solvent, in this case H_2O, is represented by an infinite homogeneous continuous medium having a dielectric constant of 78.3, and the solute is represented by an empty cavity, inside which the solute's electrostatic charge distribution is placed. This approach self-consistently minimizes the electrostatic energy by optimizing the polarization of the continuous medium and charge distribution of the solute. The cavitation and dispersion contributions to the solvation energy are less straightforward to handle because the interactions take place at short distances. There are several proposed ways to do this [71,73,75,80–84]. One of the simplest approaches for estimating these terms is to use empirically derived expressions that depend only on the solvent accessible surface area. A widely used parameterized formula of this type has been given by Sitkoff et al. [83]

$$\Delta G_{cav+disp} = \gamma A + b \quad (24)$$

where γ and b are constants set to 5 cal/mol-Å^2 and 0.86 kcal/mol, respectively. Sitkoff et al. fit the constants γ and b to the experimentally determined free energies of solvation of alkanes [85] by using a least-squares fit. A shortcoming of this model is that it is not size extensive and cannot be used to study dissociative processes. Another popular formula, which is size extensive, has been suggested by Honig et al. [82]

$$\Delta G_{cav+disp} = \gamma A \quad (25)$$

where A is the solvent accessible surface area and γ is a constant set to 25 cal/mol-Å^2. The solvent accessible surface area in Eqs. (28) and (29) is defined by using a solvent probe with a radius of 1.4 Å rolled over the solute surface defined by van der Waals radii (i.e., H=1.2 Å, C=1.5 Å, O=1.4 Å, Cl=1.8 Å). The Gaussian 98 program package [65] also contains a popular method to yield these terms. The approach here estimates these terms using expressions derived from statistical mechanical models of fluids, where the dispersion and repulsion contributions were calculated using the method of Floris et al. [71] and the cavity formation contribution was calculated using the scaled particle theory of Pierotti [80].

Calculated SCRF free energies of solvation cannot be directly compared to thermodynamic tables because the standard state in the gas phase for the SCRF model is 1 mol/L at 298.15 K rather than at 1 bar of pressure at 298.15 K. However, the SCRF model is easily changed to the usual standard state convention by using the Gibbs–Duhem relation,

$$d\left(\frac{\mu}{T}\right) = \left(\frac{U}{N}\right) d\left(\frac{1}{T}\right) + \left(\frac{V}{N}\right) d\left(\frac{P}{T}\right), \quad (26)$$

and the following formulae for a simple ideal gas.

$$P\left(\frac{V}{N}\right) = RT \tag{27}$$

$$\left(\frac{U}{N}\right) = \text{const} \times RT \tag{28}$$

Integration of Eq. (26) results in the following conversion formula

$$\mu - \mu_0 = -\text{const} \times R \ln\left(\frac{\frac{U}{N}}{\frac{U_0}{N_0}}\right) - RT \ln\left(\frac{\frac{V}{N}}{\frac{V_0}{N_0}}\right), \tag{29}$$

and evaluating with the values of $\left(\frac{V_0}{N_0}\right) = \frac{8.3144\frac{J}{\text{mol}-K}\times 298.15\,K}{\text{bar}\times 10^5\frac{\text{Pascal}}{\text{bar}}} \times 10^3\frac{\text{L}}{\text{m}^3} = 23.798\frac{\text{L}}{\text{mol}}$ and $\left(\frac{V}{N}\right) = 1.0\frac{\text{L}}{\text{mol}}$ along with $U = U_0$ gives

$$\begin{aligned}\mu - \mu_0 &= -RT \ln\left(\frac{\frac{V}{N}}{\frac{V_0}{N_0}}\right) \\ &= -\left(1.986\frac{\text{cal}}{\text{mol}-\text{K}}\right)(298.15\,\text{K}) \\ &\quad \times \ln\left(\frac{1\frac{\text{L}}{\text{mol}}}{24.798\frac{\text{L}}{\text{mol}}}\right) \\ &= 1.9\,\text{kcal/mol}.\end{aligned} \tag{30}$$

Simply adding 1.90 kcal/mol to the SCRF free energy of solvation is all that is needed to change to the usual gas-phase standard-state convention of 1 bar of pressure at 298.15 K. For charged solutes, comparisons are less straightforward [23,27,28,86]. Thermodynamic tables report free energies of formation for charged solutes or electrolytes in solution relative to $H^+_{(aq)}$, with the convention that the free energy of formation of the solvated proton is zero at every temperature [87,88].

$$\Delta G^0{}_f\left(H^+_{(aq)}\right) = 0 \tag{31}$$

This means that the absolute solvation free energy of a charged solute cannot be calculated by using thermodynamic tables. However, if the true free energy of the hydrogen electrode process

$$\frac{1}{2}H_{2(g)} \rightarrow H^+{}_{(aq)} + e^-{}_{(g)}, \quad \Delta G_{rxn} = -E^0{}_H \tag{32}$$

is known, then the solvation energy of a charged solute at 298.15 K can be found by subtracting the absolute free energy of the hydrogen electrode process, i.e.,

$$\begin{aligned}\Delta G_s\left(X^-\right) &= \Delta G^0_f\left(X^-_{(aq)}\right) - \Delta G^0_f\left(X^-_{(g)}\right) \\ &\quad + \left\{-E^0_H - \left(\Delta G^0_f\left(H^+_{(aq)}\right) + \Delta G^0_f\left(e^-_{(g)}\right)\right.\right. \\ &\quad \left.\left. -\frac{1}{2}\Delta G^0_f\left(H_{2(g)}\right)\right)\right\}\end{aligned} \tag{33}$$

Similarly, SCRF-calculated solvation energies, $\Delta G_{SCRF}\left(X^-\right)$, can be used to calculate the free energies of formation $\Delta G^0_f\left(X^-_{aq}\right)$ at 298.15 K in the electrolyte standard state used by thermodynamic tables [27].

$$\begin{aligned}\Delta G^0_f\left(X^-_{(aq)}\right) &= \Delta G_{SCRF}\left(X^-\right) + \Delta G^0_f\left(X^-_{(g)}\right) \\ &\quad - \left\{-E^0_H - \left(\Delta G^0_f\left(H^+_{(aq)}\right) + \Delta G^0_f\left(e^-_{(g)}\right)\right.\right. \\ &\quad \left.\left. -\frac{1}{2}\Delta G^0_f\left(H_{2(g)}\right)\right)\right\}\end{aligned} \tag{34}$$

The exact value for E^0_H remains unknown despite extensive experimental and computational efforts. However, Tissandier et al. [89] have recently reported a value of $\Delta G_{hyd}\left(H^+\right)$

$$H^+_{(g)} \rightarrow H^+_{(aq)} \tag{35}$$

of −263.98 kcal/mol at 298.15 K which can be used to approximate E^0_H. In addition, Zhan and Dixon [90] have also recently estimated the value of $\Delta G_{hyd}\left(H^+\right)$ by using the latest developments in electronic structure theory including solvation effects. In this work, high-level ab initio electronic structure calculations were performed by using a supermolecule-continuum approach. In the supermolecule-continuum approach, part of the solvent surrounding the solute was treated quantum mechanically and an SCRF model approximated the remaining bulk solvent. With this approach, the calculated results can systematically be improved by increasing the number of quantum mechanically treated solvent molecules. $\Delta G_{hyd}\left(H^+\right)$ at 298.15 K was calculated to be −262.4 kcal/mol in good agreement with the value of Tissandier et al. [89].

The value suggested by Tissandier et al. [89] gives an E^0_H value of 98.6 kcal/mol at 298.15 K, based on the following equation.

$$\begin{aligned}E^0_H &= \Delta G_{hyd}\left(H^+\right) + \left(\Delta G^0_f\left(H^+_{(g)}\right) - \Delta G^0_f\left(H_{2(g)}\right)\right) \\ &= -263.98 + 362.58\ \text{kcal mol}^{-1} \\ &= 98.6\ \text{kcal mol}^{-1}\end{aligned} \tag{36}$$

Using this value along with the values of $\Delta G^0_f(H^+_{(aq)})$, $\Delta G^0_f(e^-_{(g)})$,and $\Delta G^0_f(H_{2(g)})$, we can simplify Eqs. (33) and (34) as

$$\begin{aligned}\Delta G_s\left(X^-\right) &= \Delta G^0_f\left(X^-_{(aq)}\right) - \Delta G^0_f\left(X^-_{(g)}\right) \\ &\quad -98.6\,\text{kcal mol}^{-1}\end{aligned} \tag{33a}$$

$$\begin{aligned}\Delta G^0_f\left(X^-_{(aq)}\right) &= \Delta G_{SCRF}\left(X^-\right) + \Delta G^0_f\left(X^-_{(g)}\right) \\ &\quad +98.6\,\text{kcal mol}^{-1}\end{aligned} \tag{34a}$$

2.4 Reaction energies for the degradation reactions of 4,4′-DDT

With all of the calculated values described above, energetics of possible pathways can be estimated. The results shown in

Table 5 Heats of reaction (kcal/mol) for hydgrogenolysis in the aqueous phase[a,b]

DDT reactions	LDA/DZVP2	PBE96/DZVP2	B3LYP/DZVP2	PBE0/DZVP2
4, 4′-DDT + e^- → $(C_6H_4Cl)_2$–CH–CCl_2 + Cl^-	−59.10	−60.31	−61.03	−60.38
$(C_6H_4Cl)_2^{\bullet}$–CH–CCl_2 + H^+ + e^- → 4, 4′-DDD	−106.09	−106.53	−106.52	−106.63
4, 4′-DDT + e^- + H^+ → 4, 4′-DDD + Cl^-	−165.16	−166.53	−167.53	−167.00
4, 4′-DDT + OH^- → (p-$C_6H_4Cl)_2$–C=CCl_2 + H_2O + Cl^-	−29.43	−31.11	−32.22	−31.33
4, 4′-DDT + OH^- → (p-$C_6H_4Cl)_2$–CH–CCl_2OH + Cl^-	−36.56	−36.70	−37.41	−27.12
(p-$C_6H_4Cl)_2$–CH–CCl_2OH → (p-$C_6H_4Cl)_2$–CH–CCl(=O) + H^+ + Cl^-	−43.40	−45.35	−46.80	−45.36
(p-$C_6H_4Cl)_2$–CH–CCl(=O) + OH^- → (p-$C_6H_4Cl)_2$–CH–COOH	−39.90	−40.88	−39.45	−39.98
4, 4′-DDT + $2OH^-$ → (p-$C_6H_4Cl)_2$–CH–COOH + H^+ + Cl^-	−119.86	−122.93	−123.66	−122.46
$R-Cl + e^- \rightarrow R + Cl^-$ *Reactions*	LDA/6-311++ G(2d,2p)	PBE96/6-311++ G(2d,2p)	B3LYP/6-311++ G(2d,2p)	
$C_2Cl_4 + e^- \rightarrow C_2Cl_3^{\bullet} + Cl^-$	−47.16	−47.54	−46.97	
$C_2HCl_3 + e^- \rightarrow$ trans-$C_2HCl_2^{\bullet} + Cl^-$	−41.39	−41.20	−40.57	
$C_2HCl_3 + e^- \rightarrow$ cis-$C_2HCl_2^{\bullet} + Cl^-$	−41.66	−41.96	−41.38	
$C_2HCl_3 + e^- \rightarrow$ 1, 1-$C_2HCl_2^{\bullet} + Cl^-$	−36.17	−36.86	−36.88	
$trans-C_2H_2Cl_2 + e^- \rightarrow trans-C_2H_2Cl^{\bullet} + Cl^-$	−37.29	−37.98	−38.10	
$cis-C_2H_2Cl_2 + e^- \rightarrow cis-C_2H_2Cl^{\bullet} + Cl^-$	−37.32	−37.69	−37.76	
1, 1-$C_2H_2Cl_2 + e^- \rightarrow$ 1, 1-$C_2H_2Cl^{\bullet} + Cl^-$	−42.20	−41.89	−41.08	

[a] Experimental aqeuous free energies used $\Delta G_f^o(e^-) = 64.0$ kcal/mol (from $\Delta G_S = -36.6$ kcal/mol [119,120], $E_H^o = 98.6$ kcal/mol-see text), $\Delta G_f^o(Cl^-) = -31.36$ kcal/mol [88], $\Delta G_f^o(Cl^-) = -37.58$ kcal/mol [88]

[b] All values used in this table were taken from [22,24]

Table 7 are the aqueous-phase Gibbs free energies of reaction for the hydrogenolysis (Eqs. (1–3)), dehydrochlorination (Eq. (4)), and hydrolysis (Eqs. (6–8)) reactions for 4,4′-DDT and its metabolites: (p-$C_6H_4Cl)_2$–CH–CCl_3, (p-$C_6H_4Cl)_2$–CH–$CCl_2^{\bullet}$, (p-$C_6H_4Cl)_2$–CH–$CHCl_2$, (p-$C_6H_4Cl)_2$–C=CCl_2, (p-$C_6H_4Cl)_2$–CH–CCl_2OH, (p-$C_6H_4Cl)_2$–CH–CCl(=O), and (p-$C_6H_4Cl)_2$–CH–COOH. Even though differences of up to 12 kcal/mol were seen for the DDT compounds in the values of ΔH_f^o (298.15 K) predicted from different ab initio methods, the relative differences between the methods were significantly smaller. As a result, the relative energy differences and overall reaction energies were found to be consistent within a few kcal/mol. The largest standard deviation in reaction energies was 1.93 kcal/mol for the overall hydrolysis reaction (4, 4′-DDT + $2OH^-$ → (p-$C_6H_4Cl)_2$ − CH–COOH + H + Cl^-). The largest absolute difference was 4.98 kcal/mol between the SVWN5/DZVP2 and B3LYP/DZVP2 reaction energies of overall hydrolysis reaction.

Results such as this demonstrate that ab initio electronic structure methods can be used to calculate the reaction energetics of a potentially large number reactions involving organic compounds in solution, including large and complex molecules such as 4,4′-DDT for which experimental data are unavailable, and can be used to help identify the potentially important environmental degradation reactions. Finally, it is important to emphasize that the thermodynamic quantities presented here are studies to determine if a reaction is even allowed or not. Equally important in understanding these reactions are the height and shape of kinetic barriers existing between the reactants and products including the role of solvent on the reaction pathways.

3 Estimating the kinetics of dissociative electron attachment

Dissociative electron attachment (DEA) reactions, Eq. (2), involve the attachment of an electron in which a bond is simultaneously broken [9,10]. Two possible mechanisms have been identified for Eq. (2): a stepwise mechanism and a concerted mechanism [91,92]. In the stepwise mechanism, the electron transfer forms a stable radical anion intermediate that subsequently undergoes dissociation.

$$RCl + e^- \longleftrightarrow RCl^{\bullet -} \rightarrow R^{\bullet} + Cl^- \quad (37)$$

In the concerted mechanism, ET and dissociation occur simultaneously.

$$RCl + e^- \rightarrow R^{\bullet} + Cl^- \quad (38)$$

It is not known which reaction mechanism is pertinent for many PCHs, as it depends on several factors including the type of PCH, the type of solvent, and the strength of the reductant. In this section we illustrate how computational chemistry methods can be used to determine activation barriers for the concerted pathway. However, methods discussed here can be extended to characterize the stepwise mechanism.

The activation energy of a concerted DEA reaction of PCHs in the gas phase can be estimated by finding the crossing point of the dissociation potential energy curves for the neutral R–Cl and the radical anion $R–Cl^{-\bullet}$ as a function of the C–Cl bond length [32,34,93]. The physics of concerted DEA is illustrated in Fig. 3. The red curve is the dissociation potential energy surface for a generic C–Cl bond in chlorocarbons plus the energy of an electron in vacuum (which is set to zero). The binding energy varies considerably with the chlorocarbons ($\sim$ 65 kcal/mol for CCl_4 and $\sim$ 92 kcal/mol for C_2Cl_4). The blue curve is the dissociative potential energy surface for the C–Cl bond of the anion upon an attachment of an electron. The anion structure is not stable in the DEA reaction, suggesting that the electron transfer occurs when the neutral molecule adopts a structure close to the one at the crossing point, at which point it captures the electron and then dissociates into a chlorocarbon radical and a chloride ion. It should be mentioned that other reducing agents, besides the free electron, can be included into the model by simply adding a constant to the neutral curve [91,93]. Furthermore in this theory the height of the activation barrier is highly dependent on the strength of the reducing agent, where the barrier increases as the energy of the electron increases and decreases as the energy of the electron decreases. A limitation of this model is that it does not explicitly include the zero point and entropic changes associated with the other vibrational modes besides C–Cl stretch. However, the other vibrational changes that are orthogonal to the C–Cl vibrational mode ought to be small, since the primary zero point and entropic changes during the course of the reaction will be associated with C–Cl stretch.

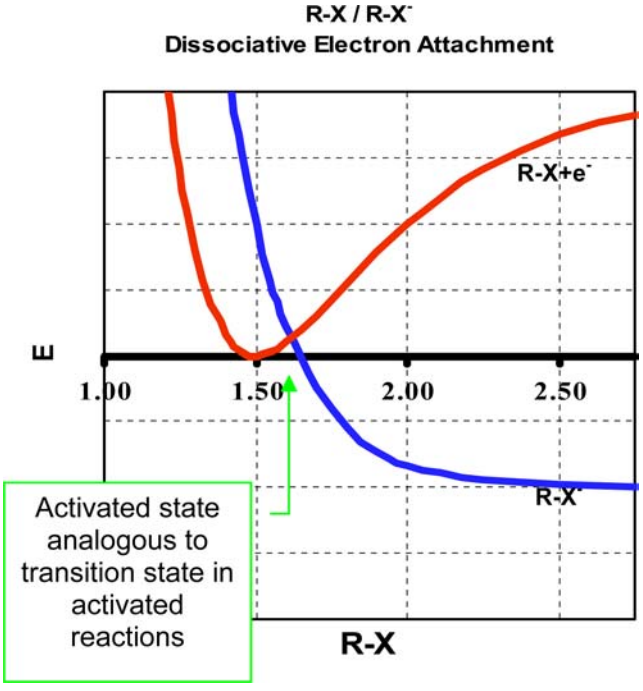

Fig. 3 Illustration of curve crossing in dissociative electron-transfer modeling

Even though the above strategy is simple, care must be taken in the choice of ab initio theory used to calculate the potential energy curves. Previous work has shown that the activation energy or "crossing point" for the DEA reaction in the gas phase is highly dependent on the ab initio level, and several authors have suggested that high-level ab initio calculations are needed in order to get accurate results [32,33, 94–96] . An example of calculated dissociation curves for the neutral and radical anion species of chloroethylene, C_2H_3Cl, at a variety of ab initio and DFT levels are shown in Fig. 4. Figure 4 shows that the level of theory does not have a significant effect on the neutral curves near the minimum (1.6 Å, . . ., 2.1 Å). The same is not true for the anion curves. This is not that surprising since it is well known that many ab initio theories fail to correctly describe the interaction between a radical and a closed shell anion. Relative to the highly accurate RCCSD(T)/aug-cc-pVTZ curve the lower-level theories have a considerable amount of error.

Interestingly, the RCCSD(T)/aug-cc-pVTZ and B3LYP/6–311++G(2d,2p) curves parallel each other. This trend is also seen for the other chlorinated ethylenes (not shown), which suggests that a correction scheme may be used to correct the B3LYP/6–311++G(2d,2p) curve. The LDA/6–311++G(2d,2p) and PBE96/6–311++G(2d,2p) curves are quite different and a simple correction scheme will not be able to generate accurate anion curves. We have found that the accuracy of anion curves can be improved by correcting for the errors in the C–Cl bond dissociation energy and the electron affinity of chlorine.

$$\begin{aligned}\Delta\chi = {} & D_e(\text{C–Cl})_{\text{high-level-theory}} \\ & - D_e\,(\text{C–Cl})_{\text{low-level-theory}} \\ & - \left(EA(\text{Cl})_{\text{exp}} - EA(\text{Cl})_{\text{low-level-theory}}\right)\end{aligned}$$

Figure 5 shows the B3LYP/6-311++G(2d,2p) and RCCSD (T)/ aug-cc-pVTZ curves using the $\Delta\chi$correction, where $D_e(C–Cl)_{\text{high-level-theory}}$ is estimated using the isodesmic reaction scheme discussed in the previous section.

It should also be mentioned that the anion curves at small distances, below the crossing point, are not accurate representations of the diabatic state. As was previously pointed out by Bertran et al. [32] and others [31,95,97–102], ab initio electronic structure calculations do not give reliable anion curves at R_{C-Cl} distances significantly smaller than the crossing point of the reaction profiles. The problem is that when the radical anion is less stable than the neutral system, the radical anion will physically prefer to be a neutral molecule plus a free electron. However, a complete switching over to the adiabatic state is not seen because the basis sets are incomplete. Rather, our results show that the anion curve plummets down and parallels the neutral curve at small distances. Following the electronic state of the anion as a function of $R_{\text{C–Cl}}$, it was found that an extra electron occupied a σ^* antibonding orbital at large distances, whereas for the nondiabatic part of the curve, a π^* antibonding orbital was occupied instead.

Solvent effects can be included by using continuum solvations models [70–75] or by explicitly adding solvent [31]. When the solvent effects are included the neutral curve is

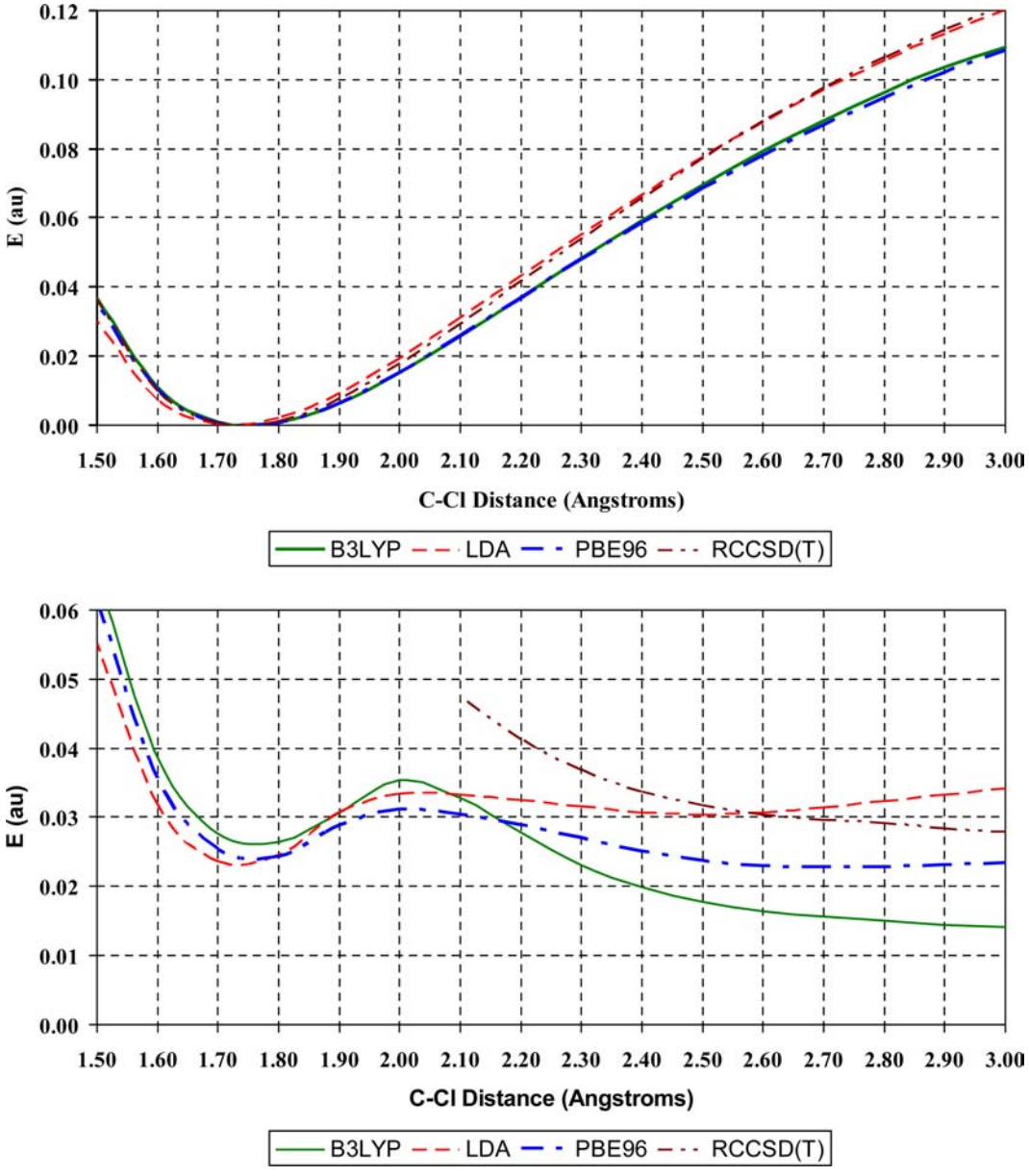

Fig. 4 Gas-phase potential energy curves for top-neutral C_2HCl_3 and bottom-radical anion $C_2HCl_3^{-\bullet}$ calculated at B3LYP/6-311++G(2*d*,2*p*), LDA/6-311++G(2*d*,2*p*), PBE96/6-311++G(2*d*,2*p*), and RCCSD(T)/aug-cc-pVTZ

not significantly affected, whereas the anion curve is dramatically stabilized [31–33,97,103]. This is expected since the solvation energy of a chloride is −75 kcal/mol. However, in aqueous reduction reactions this stabilization is countered by the energy required to extract an electron from reducing species to the gas phase, since the neutral curve was generated by setting the energy of the electron to zero. Figure 6 shows the relationship between the activation barrier and the strength of the reducing agent for aqueous C_2H_3Cl.

4 Conclusions

Molecular modeling has advanced to the point that it can be used to calculate the reaction energetics and kinetics of a potentially large number of organic compounds in solution, including radical and anionic compounds for which experimental data are unavailable, and can be used to help identify the potentially important environmental degradation reactions. In this paper, results for the thermochemical properties ΔH_f^o (298.15 K), $S°$ (298.15 K,1 bar), and ΔG_S (298.15 K, 1bar) of a large number of PCHs were presented. Furthermore, it was shown how ab initio electronic structure theory, isodesmic reactions schemes, canonical ensemble entropy formulas, and self-consistent reaction field theory can be used to reliably estimate the thermochemical properties ΔH_f^o (298.15 K), S° (298.15 K,1 bar),and ΔG_S (298.15 K, 1 bar) of PCHs. From these thermochemical data the energetics of the several degradation reactions can be estimated.

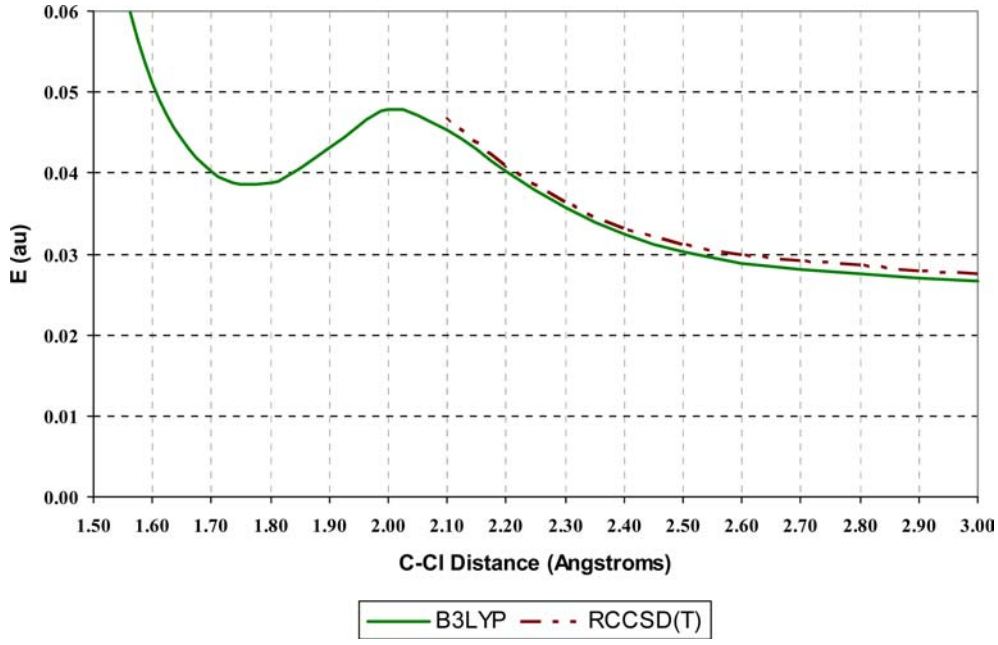

Fig. 5 Corrected gas-phase potential energy curves for radical anion $C_2HCl_3^{-\bullet}$ calculated at B3LYP/6-311++G(2*d*,2*p*) and RCCSD(T)/aug-cc-pVTZ

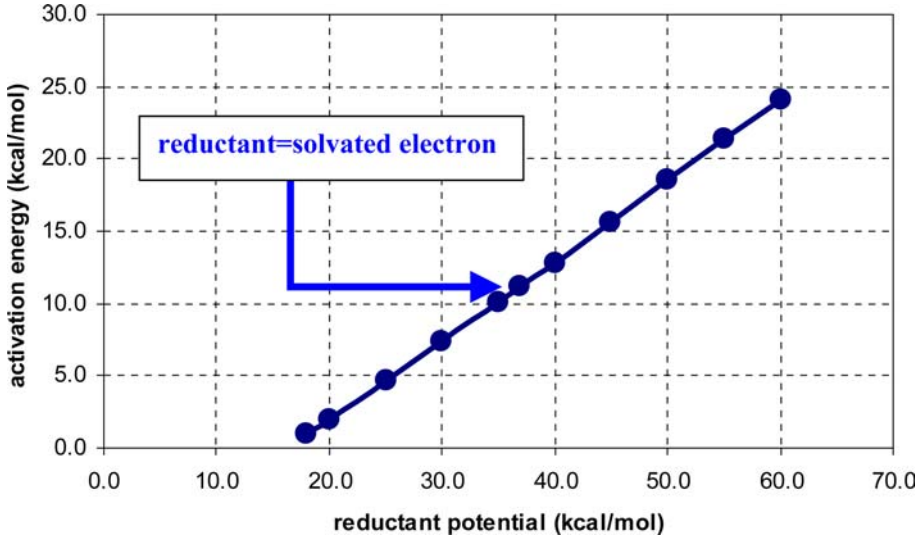

Fig. 6 Activation free energy versus the strength of the reductant for C_2H_3Cl. The reductant potential is defined as the energy taking an electron from the reductant to the gas phase (e.g., solvated electron = 34.6 kcal/mol)

A strategy for estimating the activation barrier for the concerted electron transfer reaction was also presented. In this strategy the activation energy is determined by finding the crossing point between of the dissociation potential energy curves for the neutral R–Cl and the radical anion $R–Cl^{\bullet-}$ as a function of the C–Cl bond length. The accuracy of the activation barrier was found to be highly sensitive to the level of ab initio theory. This is not that surprising since it is well known that many ab initio theories fail to correctly describe the interaction between a radical and a closed shell anion ($R–Cl^{\bullet-}$). However, we have found that the anion curve generated by lower-level B3LYP calculations parallels high-level CCSD(T) calculations and that the accuracy of the B3LYP anion curves can be improved by correcting for the errors in the C–Cl bond dissociation energy and the electron affinity of chlorine.

Acknowledgements I would like to thank David A. Dixon, Andrew R. Felmy, Michel Dupuis, and Paul G. Tratnyek for their contributions to my work in this research area. This research was supported by the Nanoscale Science, Engineering, and Technology program and the Environmental Management Sciences program of the U.S. Department of Energy, Office of Science. The Pacific Northwest National Laboratory is operated by Battelle Memorial Institute. We also wish to thank Molecular Science Computing Facility in the William R. Wiley

Environmental Molecular Sciences Laboratory (EMSL) at PNNL and the National Energy Research Scientific Computing Center at the National Energy Reasearch Scietific Computing Center (Berkeley, CA, USA).

References

1. Pankow JF, Luo WT, Bender DA, Isabelle LM, Hollingsworth JS, Chen C, Asher WE, Zogorski JS (2003) Atmos Environ 37:5023
2. Pankow JF, Cherry JA (1996) Dense chlorinated solvents and other DNAPLs in groundwater: history, behavior, and remediation. Waterloo Press, Portland
3. Mackay DM, Cherry JA (1989) Environ Sci Technol 23:630
4. Innovative Treatment & Remediation Demonstration (ITRD) Program (2002) Hanford 200 west area carbon tetrachloride project innovative remediation technology review 1999–2000, Sandi National Laboratories
5. Vogel TM, Criddle CS, McCarty PL (1987) Environ Sci Technol 21:722
6. Schwarzenbach RP, Gschwend PM, Imboden DM (1993) Environmental organic chemistry. Wiley, New York
7. Balko BA, Tratnyek PG (1998) J Phys Chem B 102:1459
8. Amonette JE, Workman DJ, Kenedy DW, Fruchter JS, Gorby YA (2000) Environ Sci Technol 34:4606
9. Wade RS, Castro CE (1973) J Am Chem Soc 95:226
10. Criddle CS, McCarty PL (1991) Environ Sci Technol 25:973
11. Curtiss GP, Reinhard M (1994) Environ Sci Technol 28:2393
12. Kriegman-King MR, Renhard M (1992) Environ Sci Technol 26:2198
13. Gaspar D, Lea A, Engelhard M, Baer D, Miehr R, Tratnyek P (2002) Langmuir 18:7688
14. Fennelly J, Roberts A (1998) Environ Sci Technol 32:1980
15. Matheson LJ, Tratnyek PG (1994) Environ Sci Technol 28:2045
16. Butler EC, Hayes KF (2000) Environ Sci Technol 34:422
17. Li T, Farrell J (2001) Environ Sci Technol 35:3560
18. Stromeyer SA, Stumpf K, Cook AM, Leisenger T (1992) Biodegradation 3:113
19. Wolfe NL, Zepp RG, Paris DF, Baughman GL, Hollis RC (1977) Environ Sci Technol 11:1077
20. Bylaska EJ, Dixon DA, Felmy AR (2000) J Phys Chem A 104:610
21. Borisov YA, Arcia EE, Mielke SL, Garrett BC, Dunning JTH (2001) J Phys Chem A 105:7724
22. Bylaska EJ, Dixon DA, Felmy AR, Apra E, Windus TL, Zhan CG, Tratnyek PG (2004) J Phys Chem A 108:5883
23. Bylaska EJ, Dixon DA, Felmy AR, Tratnyek PG (2002) J Phys Chem A 106:11581
24. Bylaska EJ, Dupuis M, Tratnyek PG (2005) J Phys Chem A 109:5905
25. Arnold WA, Wignet P, Cramer CJ (2002) Environ Sci Technol 36:3536
26. Nonnenberg C, van der Donk WA, Zipzse H (2002) Phys Rev A 106:8708
27. Patterson EV, Cramer CJ, Truhlar DG (2001) J Am Chem Soc 123:2025
28. Winget P, Cramer C, Truhlar D (2004) Theor Chem Acc 112:217
29. Perlinger JA, Venkatapathy R, Harrison JF (2000) J Phys Chem A 104:2752
30. Feller D, Peterson K, de Jong W, Dixon D (2003) J Chem Phys 118:3510
31. Soriano A, Silla E, Tunon I (2002) J Chem Phys 116:6102
32. Bertran J, Gallardo I, Moreno M, Saveant JM (1992) J Am Chem Soc 114:9576
33. Tada T, Yoshimura R (1992) J Am Chem Soc 114:1593
34. Pause L, Robert M, Saveant J (2000) J Am Chem Soc 122:9829
35. Sun H, Bozzelli JW (2001) J Phys Chem A 105:4504
36. Booty MR, Bozzelli JW, Ho WP, Magee RS (1995) Environ Sci Technol 29:3059
37. Chen C, Wong D, Bozzelli J (1998) J Phys Chem A 102:4551
38. Sun H, Bozzelli J (2003) J Phys Chem A 107:1018
39. Bartlett RJ (1989) J Phys Chem 93:1697
40. Bartlett RJ, Stanton JF (1995) In: Lipkowitz KB, Boyd DB (ed) Reviews of computational chemistry, VCH Publishers, New York
41. Kucharski SA, Bartlett RJ (1986) J Adv Quantum Chem 18:281
42. Dixon DA, Feller D, Peterson KA (1997) J Phys Chem A 101:9405
43. Peterson K, Xantheas S, Dixon D, Dunning T (1998) J Phys Chem A 102:2449
44. Kumaran S, Su M, Lim K, Michael J, Klippenstein S, DiFelice J, Mudipalli P, Kiefer J, Dixon D, Peterson K (1997) J Phys Chem A 101:8653
45. Dixon DA, Peterson KA, Francisco JS (2000) J Phys Chem A 104:6227
46. Dixon D, Feller D, Peterson K (2001) J Chem Phys 115:2576
47. Dixon D, Peterson K (2001) J Chem Phys 115:6327
48. Hohenberg P, Kohn W (1964) Phys Rev B 136:864
49. Kohn W, Sham LJ (1965) Phys Rev A140:1133
50. Vosko SH, Wilk L, Nusair M (1980) Can J Phys 58:1200
51. Becke AD (1988) Phys Rev A 38:3098
52. Perdew JP, Wang Y (1992) Phys Rev B 45:13244
53. Perdew JP, Burke K, Ernzerhof M (1996) Phys Rev Lett 77:3865
54. Adamo C, Barone V (1997) J Chem Phys 110:6158
55. Becke AD (1993) J Chem Phys 98:5648
56. Lee C, Yang W, Parr RG (1988) Phys Rev B 37:785
57. Benson SW (1968) Thermochemical kinetics; methods for the estimation of thermochemical data and rate parameters. Wiley, New York
58. Curtiss LA, Raghavachari K, Redfern PC, Pople JA (1997) J Chem Phys 106:1063
59. Curtiss LA, Raghavachari K, Trucks GW, Pople JA (1991) J Chem Phys 94:7221
60. Curtiss LA, Raghavachari K, Redfern PC, Rassolov V, Pople JA (1998) J Chem Phys 109:7764
61. Chase JMW (1998) Phys Chem Ref Data, Monograph No 9 9:1
62. Herzberg G (1947) Molecular spectra and molecular structure II. Infared and raman spectra of polyatomic molecules, D. Van Nostrand Company, New York
63. McQuarrie DA (1973) Statistical mechanics. Harper & Row, New York
64. Straatsma TP, Apra E, Windus TL, Dupuis M, Bylaska EJ, de Jong W, Hirata S, Smith DMA, Hackler MT, Pollack L, Harrison RJ, Nieplocha J, Tipparaju V, Krishnan M, Brown E, Cisneros G, Fann GI, Fruchtl H, Garza J, Hirao K, Kendall R, Nichols JA, Tsemekhman K, Valiev M, Wolinski K, Anchell J, Bernholdt D, Borowski P, Clark T, Clerc D, Dachsel H, Deegan M, Dyall K, Elwood D, Glendening E, Gutowski M, Hess A, Jaffe J, Johnson B, Ju J, R. Kobayashi R, Kutteh R, Lin Z, Littlefield R, Long X, Meng B, Nakajima T, Niu S, Rosing M, Sandrone G, Stave M, Taylor H, Thomas G, van Lenthe J, Wong A, Zhang Z (2003) NWChem, A computational chemistry package for parallel computers. Pacific Northwest National Laboratory, Richland, Washington 99352–0999, USA
65. Frisch MJ, Trucks GW, Schlegel HB, Scuseria GE, Robb MA, Chesesman JR, Zakrzewski VG, Montgomery J, J. A., Stratmann RE, Burant JC, Dapprich S, Millam JM, Daniels AD, Kudin KN, Strain MC, Farkas O, Tomasi J, Barone V, Cossi M, Cammi R, Mennucci B, Pomelli C, Adamo C, Clifford S, Ochterski J, A. PG, Ayala PY, Cui Q, Morokuma K, Malick DK, Rabuck AD, Raghavachari K, Foresman JB, Cioslowski J, Ortiz JV, Stefanov BB, Liu G, Liashenko A, Piskorz P, Komaromi I, Gomperts R, Martin RL, Fox DJ, T. K, Al-Laham MA, Peng CY, Nanayakkara A, Gonzalez C, Challacombe M, Gill PMW, Johnson B, Chen W, Wong MW, Andres JL, Gonzalez C, Head-Gordon M, Replogle ES, Pople JA (1998) Gaussian 98, Revision A.4, Gaussian, Pittsburgh, PA
66. Pitzer KS, Gwinn WD (1942) J Chem Phys 10:428
67. Zhu L, Bozzelli J, Lay T (1998) Ind Eng Chem Res 37:3497
68. McQuarrie DA (1983) Quantum chemistry. University Science Books, Sausalito, CA
69. Schokhirev NR, Program ROTATOR (http://www.chem.arizona.edu/faculty/nikolai/programs.html#programs)

70. Cossi M, Barone V, Cammi R, Tomasi J (1996) Chem Phys Lett 255:327
71. Floris FM, Tomasi J, Pascual Ahuir JL (1991) J Comput Chem 12:784
72. Miertus S, Scrocco E, Tomasi J (1981) J Chem Phys 55:117
73. Tomasi J, Persico M (1994) Chem Rev 94:2027
74. Klamt A, Schuurmann G (1993) J Chem Soc Perkin Trans 2:799
75. Cramer CJ, Truhlar DG (1999) Chem Rev 99:2161
76. Orozco M, Alhambra C, Barril X, Lopez JM, Busquest MA, Luque FJ (1996) J Mol Model 2:1
77. Cramer CJ, Truhlar DG (1992) Science 256:213
78. Cramer CJ, Truhlar DG (1995) Continuum solvation models: classical and quantum mechanical implementations. In: Lipkowitz KB, Boyd DB (ed) Reviews in Computational Chemistry 6, VCH, New York, p 1
79. Cramer CJ, Truhlar DG (1996) Continuum solvation models. In: Tapia O, Bertran J (ed) Solvent effects and chemical reactivity, Kluwer, Dordrecht, p 1
80. Pierotti RA (1965) J Phys Chem 69:281
81. Huron MJ, and P. Claverie (1974) J Phys Chem 78:1853
82. Honig B, Sharp KA, Yang A (1993) J Phys Chem 97:1101
83. Sitkoff D, Sharp KA, Honig B (1994) J Phys Chem 98:1978
84. Eckert F, Klamt A (2002) AIChE J 48:369
85. Ben-Naim A, Marcus YJ (1984) J Chem Phys 81:2016
86. Winget P, Weber E, Cramer C, Truhlar D (2000) Phys Chem Chem Phys 2:1871
87. Levine IN (1988) Physical chemistry. McGraw-Hill, New York
88. Wagman DD (1982) J Phys Chem Ref Data 11:suppl 2
89. Tissandier MD, Cowen KA, Feng WY, Gundlach E, Cohen MH, Earhart AD, Coe JV, Tuttle TR Jr. (1998) J Phys Chem A 102:7787
90. Zhan C-G, Dixon DA (2003) J Phys Chem B 107:4403
91. Costentin C, Robert M, Saveant JM (2003) J Am Chem Soc 125:10729
92. Pause L, Robert M, Saveant J (2001) J Am Chem Soc 123:4886
93. Saveant JM (1987) J Am Chem Soc 109:6788
94. Eberson L (1999) Acta Chem Scand 53:751
95. Piecuch P (1997) J Mol Struct 436–437:503
96. Roszak S, Koski W, Kaufman J, Balasubramanian K (1997) J Chem Phys 106:7709
97. Hotokka M, Roos BO, Eberson L (1986) J Chem Soc Perk T 2: 1979
98. Perez V, Lluch JM, Bertran J (1994) J Am Chem Soc 116:10117
99. Luke BT, Loew GH, McLean AD (1988) J Am Chem Soc 110:3396
100. Griffing KM, Kenney J, Simons J, Jordan KD (1975) J Chem Phys 63:4073
101. Bondybey V, Schaefer HF, Pearson PK (1972) J Chem Phys 57:1123
102. Michels HH, Harris FE, Browne JC (1968) J Chem Phys 48: 2821
103. Zhang N, Blowers P, Farrell J (2005) Environ Sci Technol 39: 612
104. Godbout N, Salahub DR, Andzelm J, Wimmer E (1992) Can J Chem 70:560
105. Dunning TH Jr (1989) J Chem Phys 90:1007
106. Kendall RA, Dunning TH, Jr, Harrison RJ (1992) J Chem Phys 96:6796
107. Peterson KA, Kendall RA, Dunning TH Jr (1993) J Chem Phys 99:1930
108. Peterson KA, Kendall RA, Dunning TH Jr (1993) J Chem Phys 99:9790
109. Woon DE, Dunning JTH (1993) J Chem Phys 98:1358
110. Woon DE, Dunning JTH (1995) J Chem Phys 103:4572
111. Barone V, Cossi M, Tomasi J (1997) J Chem Phys 107:3210
112. Chase Jr MW (1998) Phys Chem Ref Data, Monograph No 9 9:1
113. Hemmaplardh B, King JAD (1972) J Phys Chem 76:2170
114. Strauding J, Roberts PV (1996) Crit Rev Environ Sci Technol 26:205
115. Yaws CL, Yang H-C (1992) Henry's law constant for compounds in water. In: Yaws CL (ed) Thermodynamic and physical property data, Gulf Publishing Company, Houston, TX, p 181
116. Munz C, Roberts PV (1986) Environ Sci Technol 20:830
117. Clark T, Chandrasekhar J, Spitznagel GW, Schleyer PV (1983) J Comput Chem 4:294
118. Krishnan R, Binkley JS, Seeger R, Pople JA (1980) J Chem Phys 72:650
119. Coe JV (2001) Int Rev Phys Chem 20:33
120. Shiraishi H, Sunaryo GR, Ishigure K (1994) J Phys Chem 98:5164